



Full Length Article

Proteomic Approaches of *Trichoderma hamatum* to Control *Ralstonia solanacearum* Causing Pepper Bacterial Wilt

Peng Cheng^{1,2†}, Wei Song^{4†}, Xiao Gong^{1,2}, Yisong Liu³, Weiguo Xie^{1,2}, Lihua Huang^{1,2} and Yahui Hong^{1,2*}

¹Hunan Provincial Key Laboratory of Phytohormones and Growth Development, Hunan Agricultural University, Changsha 410128, PR China

²College of Bioscience and Biotechnology, Hunan Agricultural University, Changsha 410128, PR China

³National Chinese Medicinal Herbs (Hunan) Technology Center, Hunan Agricultural University, Changsha 410128, PR China

⁴Key Laboratory of Science and Engineering for Marine Ecology and Environment, The First Institute of Oceanography, SOA, Qingdao 266061, PR China

*For correspondence: cp232@163.com; cp232@sina.cn

†These authors contributed equally to this work

Abstract

Hunan province has the largest pepper cultivation and highest pepper consumption in China. In recent years, peppers (*Capsicum frutescens* L.) cultivated in Hunan province have been infected by *Ralstonia solanacearum*, causing bacterial wilt thus inducing vast economic losses. Twenty-two strains of *Trichoderma* were isolated from soil samples near the pepper cultivation area in LiLing, Hunan province, PR China. Phylogenetic analysis based on the ITS region of the isolated strains detected three species including *Trichoderma hamatum*, *T. asperellum*, and *T. virens*. An antimicrobial test showed that *T. hamatum* strain YYH13 had the greatest antimicrobial activity against the bacterial wilt pathogen and that proteins in the liquid metabolites played a major role in this activity. A 1D-shotgun proteomics approach, in conjunction with LC-MS/MS, identified 125 different secreted proteins. Most of the antimicrobial proteins contain several specific chitinases that play an important role as hydrolytic enzymes during cell wall degradation. © 2015 Friends Science Publishers

Keywords: *Trichoderma hamatum*; Antimicrobial Activity; Bacterial wilt; Pepper; Isolation and identification

Introduction

China has the largest pepper growing areas in the world. Hunan province is the leading pepper producing and consuming province in China, with a planted area of 8×10^4 hectares (Li *et al.*, 2013). Recent outbreaks of bacterial wilt have caused a sharp decrease in the pepper yield. Generally, bacterial wilt in peppers causes a 30% to 40% death rate, and in serious conditions, the rate can reach as high as 70% (Huang *et al.*, 2011). Bacterial wilt is caused by *R. solanacearum* and *Erwinia* species (Hayward, 1991). The conventional control of these pathogens has relied on chemical pesticides that are inefficient and harmful to the environment.

Trichoderma species are common fungi that make up a large portion of the soil's biomass (Samuels, 1996). They efficiently keep at least 18 genera and 20 species of pathogenic fungi and bacteria in check (Olson and Benson, 2007; Bing *et al.*, 2012; Meng *et al.*, 2013). Over the last decade, there has been an increasing demand in the agricultural market for biological agents that work with similar or possibly better efficacy than chemical agents at

defending against a wide range of plant pathogens (Yedidia *et al.*, 1999; Harman *et al.*, 2004). Consequently, the search for *Trichoderma* species with high antagonistic potential against plant pathogens has become more attractive in recent years for the development of environment friendly agricultural practices. Recently, *T. hamatum* has gained interest in both academia and industry for its ability to enhance a plant's biomass and control pathogenic fungi (Studholme *et al.*, 2013). This species' efficient control of plant pathogens depends on several physiological properties such as a rapid growth rate, ability to utilize various substrates, resistance to noxious chemicals, and production of antibiotics and extracellular hydrolytic enzymes (Carsolio *et al.*, 1994; Lorito *et al.*, 1996a, b; Kullnig *et al.*, 2000; Harman *et al.*, 2004; Chase and Fay, 2009; Studholme *et al.*, 2013). Wang *et al.* (2013) showed that *T. hamatum* could restrict the growth of bacterial wilt pathogens in ginger. Thus, research on the antimicrobial effects of *T. hamatum* will be key to determining how to control bacterial wilt in peppers.

The objective of this study was to: (1) isolate *Trichoderma* species from the soil in pepper-growing areas

contaminated with bacterial wilt; (2) analyze their morphological characteristics and phylogenetic status; (3) explain the antagonistic activity of *T. hamatum*; and (4) offer a theoretical and experimental basis for the bio-control of bacterial wilt in peppers.

Materials and Methods

Isolation of Fungi

Pepper plants infected with bacterial wilt were collected from areas in HeJiaqiao, LiLing, Hunan province, China. Soil samples were collected near the areas contaminated with bacterial wilt. *R. solanacearum* samples were obtained using a previously reported method (Wang *et al.*, 2013). First, collected soil samples were pulverized, and 5.0 g of each sample was transferred into 500 mL beakers. A 10^{-1} diluted solution was added and subsequently diluted to form 10^{-2} , 10^{-3} , 10^{-4} , 10^{-5} , 10^{-6} , 10^{-7} and 10^{-8} diluted suspensions. Diluents of each suspension were spread onto PDA (potato dextrose agar) plates and incubated at 28°C for three days, and the growth of hyphae was monitored daily.

Morphological Observations

The isolated strains were characterized by morphological analysis of mycelia and spores formed daily during the 28°C incubation. Images were taken using a Microscopic Imaging System-MVC2000 and Scanning Electron Microscope-JSM6360LV (Hause and Jahn, 2010).

PCR Amplification and Sequence Analysis

According to the manufacturer's instructions (OMEGA Bio-tek Inc., GA, USA), the primers used to identify the ITS region are described by (White *et al.*, 1990). The PCR reaction mixtures contained 4 mM MgCl₂, 5 μM of each primer, 2.5 μL of 10x reaction buffer, 0.2 mM of each dNTP, 1.25 U of Taq DNA polymerase (TAKARA), 1 μL of template DNA, and sterile distilled water for a total volume of 25 μL. The PCR program was performed using the following conditions: an initial denaturation at 94°C for 5 min; 35 cycles of 94°C for 30 s (denaturation), 55°C for 30 s (annealing), and 72°C for 30 s (extension); and a final extension at 72°C for 10 min. PCR products were visualized after electrophoresis on a 2.0% agarose gel containing ethidium bromide.

The sequencing product of the ITS1 (5'-TCGGTAGGTGATCGTGCGG-3') and ITS4 (5'-TGCACCGCTTTTTGATATGC-3') primers was examined for sequence homology among other fungi using the online program TrichOKEY (<http://isth.info/tools/molkey/index.php>) and showed relatively high similarity to the ITS sequences of isolated strains selected from the JGI database and GenBank. The neighbor-joining (NJ) method was used to construct a phylogenetic tree within the MEGA 4.1 program (Swofford, 2002).

Selection of Antagonistic Fungi Strains against Pepper Bacterial Wilt Pathogenic Bacterium and Analysis of Antimicrobial Activity of Secreted Proteins within their Liquid Metabolites (LM)

R. solanacearum suspensions were inoculated on PDA plates and cultured at 28°C for two days. Isolated *T. hamatum* strains were then inoculated on PDA plates and incubated for seven days. The antagonistic fungi strains were selected based on their growth conditions and those of *R. solanacearum*, as well as the diameter of the antagonistic fungi discs placed on each plate. *T. hamatum* strain YYH13, which displayed the best antimicrobial activity (Fig. 4), was incubated in liquid PDA medium for two days, after which its liquid metabolites (LM) were collected. *R. solanacearum* suspension spores were inoculated on a PDA plate, and four holes were then evenly punched into the plate. The liquid metabolites were inoculated into the holes and incubated at 28°C. The growth conditions of the *R. solanacearum* strains were observed after every 12 h (Fig. 1).

To analyze the main antimicrobial proteins in the LM, a (NH₄)₂SO₄ salting-out method (Kobayashi and Nakamura, 2003) was used to extract the secreted proteins. Different saturation degrees (30%, 50%, 60% and 90%) of (NH₄)₂SO₄ were prepared to precipitate the proteins. The secreted proteins were obtained by desalting and dialyzing the sediments. Analysis of the secreted proteins' antimicrobial activity at different degrees of saturation was conducted as described above.

Detection and Analysis of the Secreted Proteins

The concentrated metabolites and secreted proteins were detected by SDS-PAGE. Approximately 10 μg of protein in 2% SDS buffer solution was run through a 12.5% SDS-PAGE gel, which was then stained with Coomassie blue. SDS-PAGE gels were scanned with an Epson Perfection 4990 Photo system, and the surfaces under the optical density curves of the electrophoretic bands were calculated to determine the specified molecular weight ranges using WCIF Image J 1.37 software. Searches were performed using Mascot software, and peptides and proteins were identified using the SwissProt database (28,562 fungi proteins). We used the minimum set of protein sequences to account for all observed peptides (Nirogi *et al.*, 2007). Proteins exhibiting positive GRAVY values were recognized as hydrophobic and those with negative values were deemed hydrophilic (Kyte and Doolittle, 1982).

Gene Ontology Analysis, Signal P Prediction and PPI Analysis

We searched the GO (Gene Ontology) compartment localization information for each of the proteins identified in the LM, and the Signal P 3.0 Server (Nielsen *et al.*, 1997; Bendtsen *et al.*, 2004) was used to predict unknown proteins whose location information could not be found in the GO

database (Huai *et al.*, 2013). KEGG (Kyoto Encyclopedia of Genes and Genomes) and string network analyses were employed using DAVID Bioinformatics Resources 6.7 and String 9.05, respectively.

Results

Isolation and Identification of *Trichoderma* Strains

A total of 22 strains were isolated and maintained at 4°C on slants using the appropriate corresponding medium. Morphological analysis of the isolates identified the same group of fungi from all of the soil samples taken in the bacterial wilt areas.

Most strains had moderate colony growth with very white, dense colonies. The mycelia were white and the spore heads were green. These strains also had rapid growth rates, a thin hyphae layer, and dense mycelia that grew close to the agar surface. As exemplified by YYH13, the mycelia and spores were morphologically analyzed using photographs (Fig. 2a) and a scanning electron microscope (Fig. 2b), which suggested that YYH13 belonged to the *Trichoderma* species. Strain identification was verified by analysis of the ITS sequence.

The data formed three clades, indicating three genetic lineages of *T. hamatum*, *T. asperellum*, and *T. virens* (Fig. 3). The isolates YYH01, YYH02, YYH06, YYH08, YYH09, YYH12, YYH13, YYH14, YYH15, YYH16, YYH17, YYH18, YYH19, YYH20, YYH21 and YYH22 fell into the *T. hamatum* clade, which was sister to the *T. asperellum* clade. Strains YYH04, YYH05, and YYH10 were found to belong to the *T. asperellum* clade. All *T. virens* sequences, including strains YYH03, YYH07, and YYH11, were grouped together and formed a monophyletic clade, which was sister to the large *Trichoderma* clade.

Antimicrobial Activities of *T. hamatum* Strains

According to the antagonistic experiment, 10 of the 16 *T. hamatum* strains, including YYH01, YYH06, YYH08, YYH12, YYH13, YYH14, YYH18, YYH19, YYH20, and YYH22, proved positive for antagonistic activity. This experiment proved that these 10 strains could restrict the growth of *R. solanacearum*. The diameters of the antagonistic circles were different due to different antagonistic activities. Fig. 4A shows the diameter of the YYH13 strain's circle as the largest of the 10 strains, whereas the YYH16 strain did not display antagonistic activity (Fig. 4B). Thus, these two strains were selected as the main antagonistic control groups for this study, and the *T. hamatum* YYH13 strain was deposited in the China Center for Type Culture Collection under the accession number CCTCC M2013234.

Fig. 4C shows the antagonistic activity of the YYH13 strain's liquid metabolites in relation to the growth of *R. solanacearum*. Transparent circles could be clearly seen on

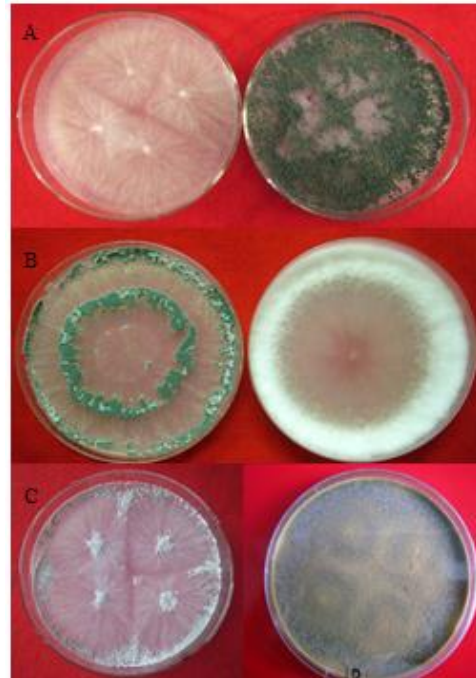


Fig. 1: Phenotype of antagonistic fungi on the PDA plate. (A, B, C): The different stages of the strains



Fig. 2: The result of electronic microscope scanning of strains. (A): mycelium; (B): spore

the culture plate, and the circles' transparency became apparent when compared to nearby holes. As the distance from the hole increased, the antagonistic effects decreased and *R. solanacearum* growth became denser. This result shows that the liquid metabolites from the *T. hamatum* strains played a key role in the antagonistic activity. Fig. 4D shows that while secreted proteins from YYH13 formed large circles, secreted proteins from YYH16 were not effective inhibitors of *R. solanacearum* growth. This result indicates that *T. hamatum* strain YYH13 produced a protein capable of restricting the growth of pathogenic bacterial wilt.

Identification of Known and Potential Antagonistic Factors in the *T. hamatum* Secretomes

As shown in Fig. 5, clear bands were observed in the No. 5 and No. 6 group samples approximately 40–50 kDa and 20–30 kDa. As described above, we found that proteins

from YYH13 had a more effective antimicrobial function.



Fig. 3: Phylogenetic tree determined by analysis of ITS sequences of *Trichoderma* species isolated from the soil in Liling, Hunan province, China. Numbers at the nodes were bootstrapping support values larger than 50% after 1000 replicates in neighbor-joining analyses. The inferred clades were labeled

Thus, we conclude that the YYH13 secretome contained proteins with a molecular weight of 40–50 and 20–30 kDa, which were able to restrict the growth of pathogenic bacteria.

As shown in Fig. 5, both *Trichoderma* strains contained multiple proteins. To identify them, bands No. 5 and No. 6 were excised and analyzed by mass spectrometry. Proteomic analysis was performed by comparing the *T. hamatum* secretome with known fungal proteomes, leading to the identification of 125 different proteins. According to GO analysis, 47% of the proteins are involved in molecular function, 8% represent cellular components, and 45.2% are involved in biological processing (Fig. 6). Of the 125 identified proteins from the LM, 39 (31.2%) are secreted or extracellularly localized and 42 (33.6%) are predicted but have not yet undergone further characterization or been assigned to a specific GO analysis category. We used the SignalP tool to predict the identity of the unknown proteins and found that 18 proteins (42.8% of unknown and 14.7% of the fully identified proteins) contained amino acids that formed part of a signal peptide (Fig. 7A). Other portions of these proteins contained sequences that identified them as

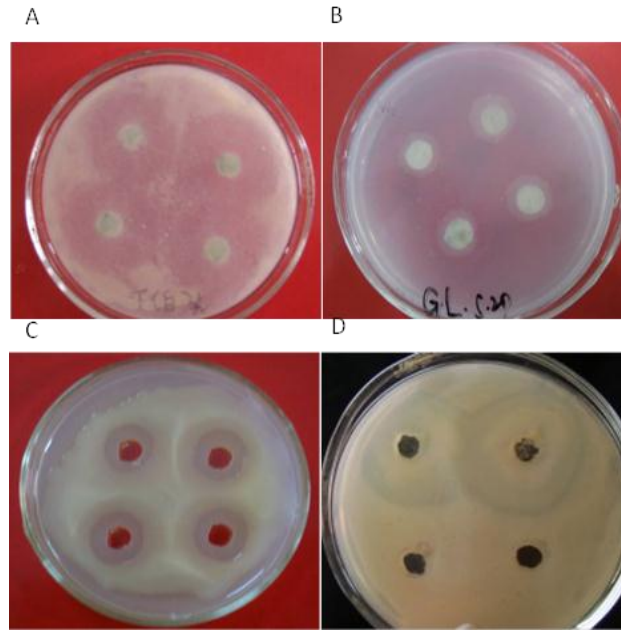


Fig. 4: Antagonistic effect of different *T. hamatum* strains and to YYH13 liquid metabolites to BW. (A):antagonistic circles emerged by YYH13 strain; (B): without antagonistic circles emerged by YYH16 strain; (C): antagonistic circles emerged by YYH13 liquid metabolites; (D): the upper half was the antagonistic circles emerged by YYH13 secreted protein, the lower half show that the YYH16 secreted protein did not have the antagonistic activity to BW

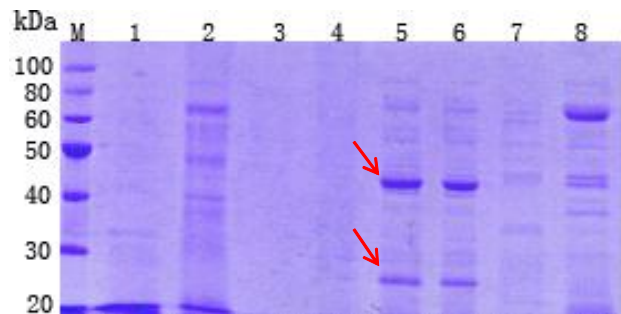


Fig. 5: SDS-PAGE of protein precipitation. (M,Marker;1,YYH01;2,YYH06; 3,YYH08; 4,YYH12; 5,YYH13; 6,YYH13; 7,YYH16; 8,YYH22)

DNA-binding proteins (1%), nucleic acid-binding proteins (6.2%), myosin (4%), ribosomal proteins (2.2%), cytoskeletal proteins, microtubule proteins (7.3%), nuclear proteins (6.2%), microsomal proteins (0.7%), endoplasmic reticulum proteins (1.4%), cytoplasmic proteins (4.1%), mitochondrial proteins (1.9%), and membrane-associated proteins (2.4%). Understandably, genes encoding these functions may be more conserved across different species and are thus easier to annotate in the database.

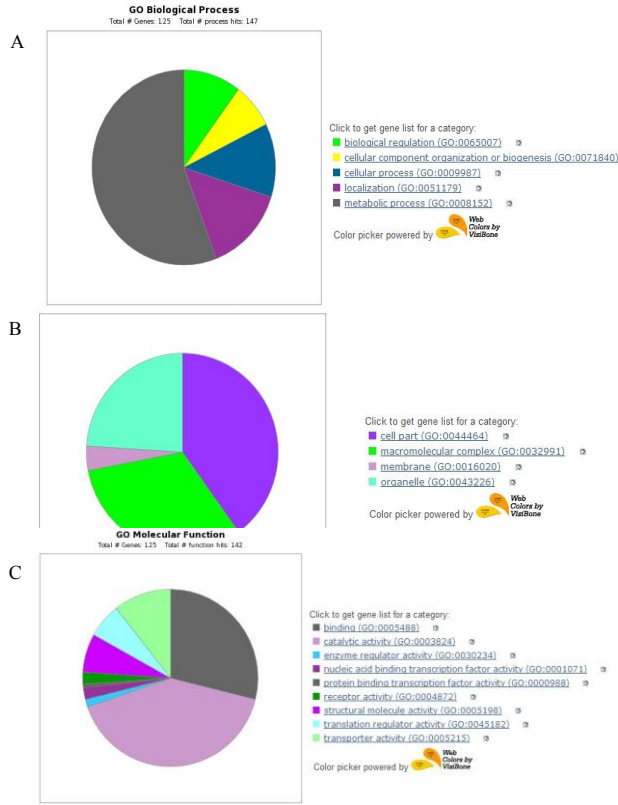


Fig. 6: Proteins identified were associated with their molecular functions by gene ontology (GO) process annotations using Panther algorithm. Protein abbreviations correspond to Entrez Gene identifiers. (A): Biological process analysis; (B): Cellular component; (C): Molecular function

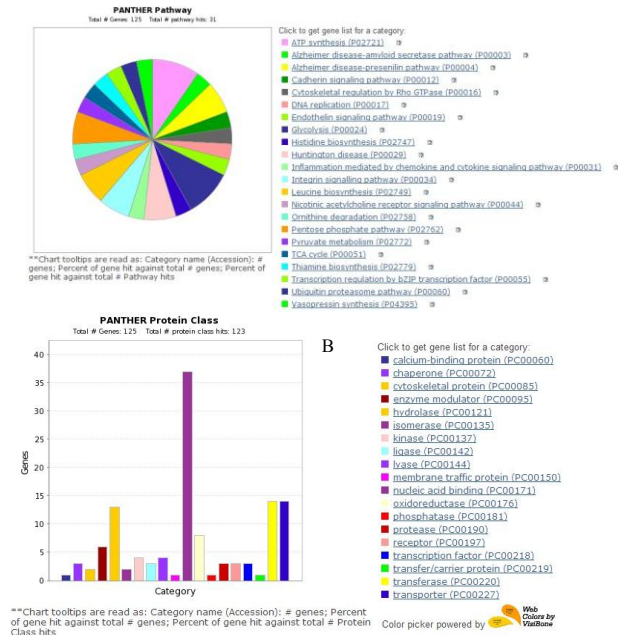


Fig. 7: Signal pathway analysis of differential proteins. (A): Panther pathway; (B): Protein class

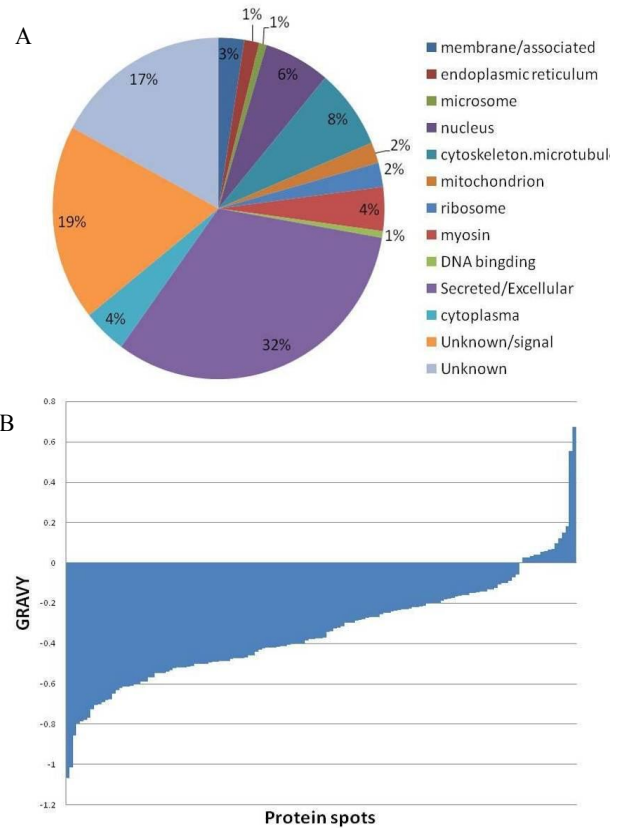


Fig. 8: Primary subcellular localization and of the identified proteins. (A): The location information is from the GO database and Swiss-Prot and TrEMBL. The unknown protein, which cannot locate from both databases is predicted by SignalP tool. (B): The average hydrophobicity was calculated using the ProtParam software. The proteins exhibiting positive GRAVY values were recognized as hydrophobic and those with negative values were deemed hydrophilic

Peptide fragments IVLGMPIYGR and ELISFDTPDMINTKVAYLK are homologous with endochitinase 42 of *T. harzianum*, *T. asperellum*, *T. longibrachiatum*, *T. virens*, *T. atroviride*, *T. velutinum*, *T. oblongisporum*, *T. voglmayrii*, *T. tomentosum*, *T. minutisporum*, *Hypocrea pilulifera* and *H. lacuwombatensis* and chitinase 18-18 of *T. citrinoviride* (Table 1). Moreover, five peptide homologs were predicted by developing analytical peptide fragments GSVANM SLGGGK, VAVVAGFGDVGK, and GSVANMSLAGAK (Table 2).

Altogether, these proteins were clearly identified and found to be quantitatively dominant in our study. Further studies will clarify the role of these secreted proteins, especially because the 40-50 kDa protease could restrain the growth of *R. solanacearum*. In contrast to YYH13, proteins secreted from YYH16 were not antagonistic, suggesting a difference in antagonistic mechanisms between the two strains.

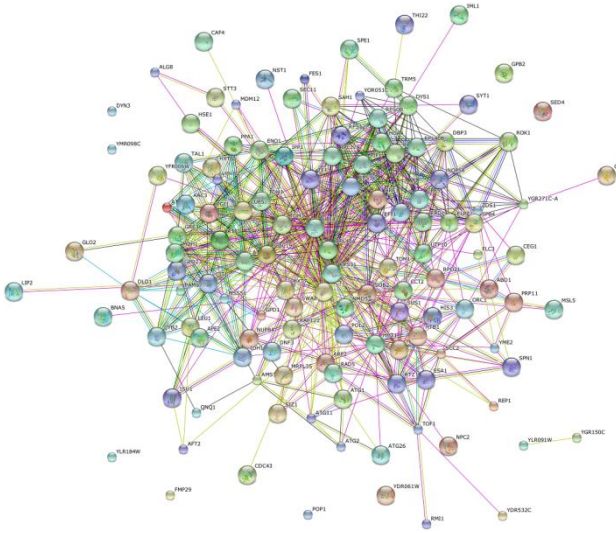


Fig. 9: The STRING network analysis of the LM proteins. Colored lines between the proteins indicate the various types of interaction evidence. Protein nodes which are enlarged indicate the availability of 3D protein structure information

Bioinformatic Analysis of the Identified Proteins

The unique sequences within the identified proteins were subjected to KEGG analysis to define metabolic pathways associated with these proteins. As expected, some putative enzymes belonging to fungi were associated with the metabolism of amino and nucleotide sugars. COG assignments were used to predict and classify possible functions of these unique sequences. Based on sequence homology, these unique sequences were classified into 22 COG categories (Fig. 7A) including ATP synthesis, glycolysis, and integrin signaling pathway. In the Panther protein class, nucleic acid binding, transferase, transporter, hydrolase, and oxidoreductase categories were most commonly assigned, accounting for 68.8% of the total assignments (Fig. 7B).

Proteins exhibiting positive GRAVY values are hydrophobic and those with negative values were deemed GRAVY values calculated in our study varied from -1.0692 to 0.6741, and 149 (88.7%) of them were negative (Fig. 8B). Thus, most of our identified proteins are hydrophilic, which are likely secreted into the extracellular matrix and function as growth factors or cell signaling molecules.

As shown from the STRING network analysis of the secreted LM proteins (Fig. 9), each circle represents a protein; the spatial distance closer to the protein represents a single class. Interactions between the most closely related proteins were also identified and assigned values; these proteins included SPE1, ARF1, HIS3, AMS1, HHT1, TEF1,

and TOM1. These proteins are mainly involved in functions such as cell cycle regulation, cell growth, apoptosis, senescence, signal transduction, protein decomposition, metabolism, transport, and glycosylation.

Discussion

From 1984 to 1991, *Trichoderma* was divided into five groups, *Pachybasium*, *Longibrachiatum*, *Trichoderma*, *Hypocreanum*, and *Saturnisporum* (Bissett, 1991; Bissett, 1992; Kullnig *et al.*, 2000), named according to their morphological characteristics. *Trichoderma* species were traditionally classified according to the characteristics of their conidia, conidiophores, and phialides (Rifai, 1969). However, their morphological characteristics can change as culture conditions vary. Thus, more and more studies began to use molecular biology techniques to identify fungi. Kullnig *et al.* (2002) used four different gene loci to study the phylogenetic relationships of *Trichoderma* and reclassified *Hypocreanum* as *Pachybasium*. Chen *et al.* (1999) analyzed soluble proteins from six species of bacteria (26 strains) by polyacrylamide gel electrophoresis and found that the electropherogram patterns of intraspecific proteins were significantly different, whereas the electropherogram patterns of interspecific proteins were similar. In this study, 22 strains of wild *Trichoderma* species were isolated using morphological and molecular identification. The strains were divided into three groups: 16 strains belonging to *T. hamatum*, three strains belonging to *T. asperellum* and the rest belonging to *T. virens*.

Trichoderma species are widely used in the biological control of plant pathogens. Kullnig *et al.* (2000) found that *T. harzianum* could effectively control *Erwinia* species and *R. solanacearum*, which causes disease in ginger plants. Harman *et al.* (2004) found that *T. harzianum* could control maize anthracnose caused by *Colletotrichum graminicola*. Badri *et al.* (2007) showed that *T. harzianum* had an inhibitory effect on the pathogens *Fusarium oxysporum* and *F. moniliforme* as determined by dual culture experiments. In the past few years, with the development of the microbe associated molecular patterns (MAMPs) theory, studies on the mechanism of the antimicrobial activity of *Trichoderma* have been brought to the forefront. Lorito *et al.* (1996a) showed that *T. harzianum* could produce hundreds of antimicrobial secondary metabolites and further identified the antimicrobial peptides in the metabolites. Four peptaibols, biologically active peptides, in the *T. harzianum* fermentation liquor were isolated and identified by Iida *et al.* (1994). They had strong inhibitory effects against *Thanatephorus cucumeris*, *Rhizoctonia solani*, *F. oxysporum* and *Magnaporthe oryzae*. In this study, the secreted proteins in the *T. hamatum* fermentation liquor were effective at controlling *R. solanacearum*. However, research is very limited with respect to the antimicrobial effectiveness of secondary metabolites of *T. hamatum*.

Extracellular products, especially secreted proteins, enter into direct contact with host cells and play a major role

Table 1: The MS/MS analysis results of parts protein

Protein name	Accession	Protein mass	Peptide No	Sequence Coverage%	PI	Peptide mass	Peptide sequence
Endochitinase	P48827	46085	5	9	7.01	810.4310	TAITFMK
						1117.6318	IVLGMPIYGR
						1270.6744	NFAKTAITFMK
						1638.7811	ELISFDTPDMINTK
						2213.1290	ELISFDTPDMINTKVAYLK
Alkaline protease 2	B0Y473	52779	3	5	5.81	948.4341	AYFSNYGK
						1076.5284	GSVANMSLGGGK
						1128.5451	HPDVEYIEK
Adenosylhomocysteinase	O13639	47866	1	2	5.61	1117.6132	VAVVAGFGDVGK
Ubiquitin-40S ribosomal protein	P0C016	17475	5	35	9.78	764.4255	MQIFVK
						1066.6135	ESTLHLVLR
						1080.5451	TLSDYNIQK
						1522.7740	IQDKEGIPPDQQR
						1762.8836	TITLEVESSDTIDNVK
Imidazoleglycerol-phosphate dehydratase	P34041	22684	5	31	5.83	927.5502	ALGALTGVA
						1571.7620	FGYAYAPLDEALSR
						1958.0837	AVVDLSNRPYTVVDLGLK
						2114.1848	AVVDLSNRPYTVVDLGLKR
						2364.2624	SQVISINTGIGFLDHMLHALAK
Glyceraldehyde-3-phosphate dehydrogenase	Q00584	36121	3	13	8.26	818.4399	VGINGFGR
						1384.7310	GAAQNIIPSSTGAAK
						1494.8406	VPTPNVSVVDLTVR
Amino peptidase 2	Q59KZ1	104873	2	2	5.19	1006.5699	FTISLIAD
						1712.8257	ADEINQIFDAISYSK
Subtilisin-like protease pepC	serine P33295	57142	2	3	6.82	713.3279	MPSSHR
						1092.5234	GSVANMSLAGAK

Table 2: Comparison results of antibacterial peptide of homologous

Number	Accession	Alignment Result	Sequence
Number 1, Similarity percentage: 42.85 %	AP00434	GLMSV LGH AVGN+VLGG LFKS	G++SV+++A++NMSLGG+GK+
Number 2, Similarity percentage: 40 %	AP00794	IIGPV LGM VGSALGG LLLK KI	++GSVANM++S+LGG++GK+
Number 3, Similarity percentage: 40 %	AP00605	+ILPILSLIGGLLGK	GSVANMSL+GG++GK
Number 4, Similarity percentage: 40 %	AP00598	FLS+AITS L+LGKLL	+GSVANMSLGGGK++
Number 5, Similarity percentage: 40 %	AP00525	ILGPVLSM VGSALGG LIIK KI	++GSVANM++S+LGG++GK+
Number 6, Similarity percentage: 38.46 %	AP01481	+A++AGM GFFGAR	VAVVAGFGDVG+K
Number 7, Similarity percentage: 35.71 %	AP00336	+AERV GAG+APVYL	VA++VVAGFGDVGK
Number 8, Similarity percentage: 35.29 %	AP02118	FLPAALAGIGG ILGKLF	++VAVVAG+FGDVGK++
Number 9, Similarity percentage: 35 %	AP00503	FLGPV VFKLASKVFP AVFGKV	+VAVV+++A++GFGDV+GK+
Number 10, Similarity percentage: 33.33 %	AP01805	+A+W KLF+DDG V	VAVVAGFGDVGK
Number 11, Similarity percentage: 42.85 %	AP00434	GLMSV LGH AVGN+VLGG LFKS	G++SV+++A++NMSLGG+GK+
Number 12, Similarity percentage: 40 %	AP00794	IIGPV LGM VGSALGG LLLK KI	++GSVANM++S+LGG++GK+
Number 13, Similarity percentage: 40 %	AP00605	+ILPILSLIGGLLGK	GSVANMSL+GG++GK
Number 14, Similarity percentage: 40 %	AP00598	FLS+AITS L+LGKLL	+GSVANMSLGGGK++
Number 15, Similarity percentage: 40 %	AP00525	ILGPVLSM VGSALGG LIIK KI	++GSVANM++S+LGG++GK+

in the antagonistic effect of fungi. As a consequence, research on secretomes is of particular relevance to identifying proteins involved in the biological control process, and several studies have been carried out for different pathogens in recent years (Wang *et al.*, 2013). Using proteomic analysis, we identified a total of 125 non-redundant secreted proteins in the liquid metabolites of YYH13. GO analysis revealed that approximately 50% of these proteins are secreted proteins or are proteins located

in the extracellular matrix. They contained an amino acid residue, IVLGMPIYGR, with 100% homology to endochitinase (Gruber *et al.*, 2011; Loc *et al.*, 2011). SDS-PAGE followed by in-gel digestion effectively removed any remaining phenolsulfonphthalein and other contaminants within the LM, which could have affected mass spectrometry results. A 1D-shotgun approach and LC-MS/MS showed that most of the antimicrobial proteins were secreted, along with other molecules. Therefore, these

results indicate that our 1D-shotgun approach, in conjunction with previous cell purification and protein identification research, was effective.

We decided to focus on LM proteins actively secreted by YYH13 because they were known to have antimicrobial activity. To further understand the roles these proteins, we generated a matrix of their biological associations, which shows the distribution of LM proteins across biological processes and the same proteins across molecular functions (Lorito *et al.*, 1996b). This technique was more sensitive than a two-dimensional gel approach in detecting proteins present at low levels.

Using GO analysis, we constructed a map of the biological processes, molecular functions, and cellular components to which these proteins were assigned. Most of the proteins identified were assigned to one or more biological categories. We also noted interesting differences between the protein bands separated by SDS-PAGE. Approximately 255 proteins between 40 and 50 kDa were identified, representing 121 gene families. Likewise, 164 proteins between 20 and 30 kDa were identified, belonging to 120 different gene families. However, individual proteins rarely function on their own; it is their interactions that form the complex networks that are responsible for almost all cellular processes. Therefore, we used the STRING network to identify key protein-protein interactions, and several proteins become part of core pathway clusters. Various strategies have been used to store these data to ease retrieval and analysis of protein-protein interaction (PPI) networks. From the PPI analysis, we determined that several proteins are at the nodes of some core clusters. Most of these proteins are enzymes belonging to several different biosynthesis pathways, and we speculate that metabolic processes may be important to their regulatory activities.

In this study, it should be noted that in contrast to YYH16, the YYH13 secretome contains several specific chitinases, underscoring the role of chitin as a carbon source in the environment. In fact, chitin synthase and chitinase play an important role as hydrolytic enzymes for plant cell wall degradation (Loc *et al.*, 2011). Therefore, chitinases may be especially relevant to the biological control activity of YYH13.

Finally, although we identified a number of proteins and thousands of peptide sequences, this study does not represent a complete analysis of the proteome of *T. hamatum*. Nevertheless, this method clearly provides a large-scale analysis of the proteome of this organism. In addition, we have developed a successful procedure for protein sample preparation that could prove useful in future proteomic analyses. This method requires further improvements and optimization, but the experimental setup proposed in this study generated a greater number of protein identifications than both 2-DE and MS analysis combined.

Conclusion

One hundred and twenty five proteins of the *T. hamatum* secretome were identified. An antimicrobial test showed that *T. hamatum* strain YYH13 had the greatest antimicrobial activity against the bacterial wilt pathogen and that proteins in the liquid metabolites played a major role in this activity. Most of the antimicrobial proteins contain several specific chitinases that play an important role as hydrolytic enzymes during cell wall degradation.

Acknowledgements

This work was supported by NSFC-Shandong Joint Funded Project "Marine Ecology and Environmental Sciences" (no.U1406403), the Ministry of Agriculture '948' project (2013-Z58) and College students innovative experiment plan of Hunan province(SCX1419)

References

- Badri, M., M.R. Zamani and M. Motallebi, 2007. Effect of plant growth regulators on in vitro biological control of *Fusarium oxysporum* by *Trichoderma harzianum* (T8). *Pak. J. Biol. Sci.*, 10: 2850–2855
- Bendtsen, J.D., H. Nielsen, G. Heijne and S. Brunak, 2004. Improved prediction of signal peptides: SignalP 3.0. *J. Mol. Biol.*, 340: 783–795
- Bissett, J., 1991. A revision of the genus *Trichoderma* II: Intraspecific classification. *Can. J. Bot.*, 69: 2357–2372
- Bissett, J., 1992. *Trichoderma atroviride*. *Can. J. Bot.*, 70: 639–641
- Bing, L., F.L. Jian, A. Ying, J. Qu, Z. Li, J. Su, Y. Zhang, J. Liu, D. Feng, K. Qi, Y. He, J. Wang and H.B. Wang, 2012. Lysin Motif-Containing Proteins LYP4 and LYP6 Play Dual Roles in Peptidoglycan and Chitin Perception in Rice Innate Immunity. *Plant Cell*, 24: 3406–3419
- Carsolio, C., A. Gutiérrez, B. Jiménez, M.M. Van and E.A. Herrera, 1994. Characterization of *ech-42*, a *Trichoderma harzianum* endochitinase gene expressed during mycoparasitism. *Proc. Natl. Acad. USA*, 91: 10903–10907
- Chase, M.W. and M.F. Fay, 2009. Barcoding of plants and fungi. *Science*, 325: 682–683
- Chen, J.A., W.M. Wang and W.J. Chen, 1999. *Trichoderma* spp. by soluble protein gel electrophoresis analysis. *Chin. J. Biol. Cont.*, 15: 77–80
- Gruber, S., C.P. Kubicek and V. Seidl, 2011. Differential regulation of orthologous chitinase genes in mycoparasitic *Trichoderma* species. *Appl. Environ. Microbiol.*, 77: 7217–7226
- Hause, G. and S. Jahn, 2010. Preparation of fungi for ultrastructural investigations and immunogold labelling. *Methods Mol. Biol.*, 638: 291–301
- Harman, G.E., C.R. Howell, A. Viterbo, I. Chet and M. Lorito, 2004. *Trichoderma* species-opportunistic, avirulent plant symbionts. *Nat. Rev. Microbiol.*, 2: 43–56
- Hayward, A.C., 1991. Biology and epidemiology of bacterial wilt caused by *Pseudomonas solanacearum*. *Annu. Rev. Phytopathol.*, 29: 65–87
- Huang, Z.N., J.H. Wen and W.Fu, 2011. Status of hot pepper production in Hunan and green control of diseases and insect pests in the crop. *J. China Capsicum*, 4: 43–45
- Huai, Mi., M. Anu and D. Paul, 2013. PANTHER in 2013: modeling the evolution of gene function, and other gene attributes, in the context of phylogenetic trees. *Nucl. Acids. Res.*, 41: 377–386
- Iida, A., M. Sanekata, T. Fujita, H. Tanaka, A. Enoki, G. Fuse, M. Kanai, P.J. Rudewicz and E. Tachikawa, 1994. Fungal metabolites. XVI. Structures of new peptaibols, trichokindins I-VII, from the fungus *Trichoderma harzianum*. *Chem. Pharm. Bull.*, 42: 1070–1075

- Kobayashi, F. and Y. Nakamura, 2003. Efficient production by *Escherichia coli* of recombinant protein using salting-out effect protecting against proteolytic degradation. *Biotechnol. Lett.*, 25: 779–782
- Kullnig, C., R.L. Mach, M. Lorito and C.P. Kubicek, 2000. Enzyme division from *Trichoderma atroviride* (= *T. harzianum* P1) to *Rhizoctonia solani* is a prerequisite for triggering of *Trichoderma ech42* gene expression before mycoparasitic contact. *Appl. Environ. Microbiol.*, 66: 2232–2234
- Kullnig, C.M., G. Szakacs and C.P. Kubicek, 2002. Phylogeny and evolution of the genus *Trichoderma*: a multigene approach. *Mycological Res.*, 106: 757–767
- Kyte, J. and R.F. Doolittle, 1982. A simple method for displaying the hydropathic character of a protein. *J. Mol. Biol.*, 157: 105–132
- Li, X., Y. Xie, J. Wang, G. Christakos, J. Si, H. Zhao, Y. Ding and J. Li, 2013. Influence of planting patterns on fluoroquinolone residues in the soil of an intensive vegetable cultivation area in northern China. *Sci. Total Environ.*, 458: 63–69
- Loc, N.H., H.T. Quang, N.B. Hung, N.D. Huy, T.T. Phuong and T.T. Ha, 2011. *T. asperellum Chi42* Genes Encode Chitinase. *Mycobiology*, 39: 182–186
- Lorito, M., V. Farkas, S. Rebu Vat, B. Bodo and C.P. Kubicek, 1996a. Cell wall synthesis is a major target of mycoparasitic antagonism by *Trichoderma harzianum*. *J. Bacteriol.*, 178: 6382–6385
- Lorito, M., R.L. Mach, P. Sposato, J. Strauss, C.K. Peterbauer and C.P. Kubicek, 1996b. Mycoparasitic interaction relieves binding of the Cre1 carbon catabolite repressor protein to promoter sequences of the *ech42* (endochitinase-encoding) gene in *Trichoderma harzianum*. *Proc. Natl. Acad. Sci. USA*, 93: 14868–14872
- Meng, F., D. Wei and W. Wang, 2013. Heterologous protein expression in *Trichoderma reesei* using the *cbhII* promoter. *Plasmid*, 54: 158–169
- Nielsen, H., J. Engelbrecht, S. Brunak and H.G. Von, 1997. Identification of prokaryotic and eukaryotic signal peptides and prediction of their cleavage sites. *Protein Eng.*, 10: 1–6
- Nirogi, R., K. Mudigonda and V. Kandikeke, 2007. Chromatography-mass spectrometry methods for the quantitation of statins in biological samples. *J. Pharm. Biomed. Anal.*, 44: 379–387
- Olson, H.A. and D.M. Benson, 2007. Induced systemic resistance and the role of binucleate *Rhizoctonia* and *T. hamatum* 382 in biocontrol of Botrytis blight in geranium. *Bio Cont.*, 42: 233–241
- Rifai, M.A., 1969. A revision of the genus *Trichoderma*. *Mycol. Papers*, 116: 1–56
- Samuels, G.J., 1996. *Trichoderma*: a review of biology and systematics of the genus. *Mycol. Res.*, 100: 923–935
- Studholme, D.J., B. Harris, K.L. Cocq, R. Winsbury, V. Perera, L. Ryder, J.L. Ward, M.H. Beale, C.R. Thornton and M. Grant, 2013. Investigating the beneficial traits of *Trichoderma hamatum* GD12 for sustainable agriculture—insights from genomics. *Front. Plant Sci.*, 4: 1–13
- Swofford, D.L., 2002. PAUP*: Phylogenetic Analysis Using Parsimony (and Other Methods). Sinauer Associates, Sunderland, Massachusetts, USA
- Wang, S.L., X. Gong, S.D. Zhou, P. Cheng and Y.H. Hong, 2013. The isolation and identification of ginger blast pathogen and screening of its antagonistic fungus. *J. Hunan. Agric. University*, 39: 282–285
- White, T.J., T. Bruns and S. Lee, 1990. *Amplification and Direct Sequencing of Fungal Ribosomal RNA Genes for Phylogenetics PCR Protocols: A Guide to Methods and Applications*, Vol. 22, pp: 315–322. Academic Press Inc., New York, USA
- Yedidia, I., N. Benhamou and I. Chet, 1999. Induction of defense responses in cucumber plants (*Cucumis sativus* L.) by the biocontrol agent *Trichoderma harzianum*. *Appl. Environ. Microbiol.*, 65: 1061–1070

(Received 03 April 2015; Accepted 07 May 2015)